

Multiscale characterization of anammox granules and microbial migration Under variable nitrogen loading rates

Article

Published Version

Creative Commons: Attribution 4.0 (CC-BY)

Open Access

Fan, X., Qian, Y., Yang, X., Wang, Y., Yang, H. ORCID: <https://orcid.org/0000-0001-9940-8273> and He, S. (2025) Multiscale characterization of anammox granules and microbial migration Under variable nitrogen loading rates. *Water*, 17 (11). 1653. ISSN 2073-4441 doi: 10.3390/w17111653 Available at <https://centaur.reading.ac.uk/123294/>

It is advisable to refer to the publisher's version if you intend to cite from the work. See [Guidance on citing](#).

To link to this article DOI: <http://dx.doi.org/10.3390/w17111653>

Publisher: MDPI

All outputs in CentAUR are protected by Intellectual Property Rights law, including copyright law. Copyright and IPR is retained by the creators or other copyright holders. Terms and conditions for use of this material are defined in the [End User Agreement](#).

www.reading.ac.uk/centaur


CentAUR

Central Archive at the University of Reading

Reading's research outputs online

Article

Multiscale Characterization of Anammox Granules and Microbial Migration Under Variable Nitrogen Loading Rates

Xiaoliang Fan ^{1,2}, Yunzhi Qian ², Xueying Yang ¹, Yilin Wang ¹, Hong Yang ³  and Shilong He ^{2,*}¹ State Key Laboratory of Petroleum Pollution Control, Beijing 102206, China² School of Environment and Spatial Informatics, China University of Mining and Technology, Xuzhou 221116, China³ Department of Geography and Environmental Science, University of Reading, Reading RG6 6AB, UK; h.yang4@reading.ac.uk

* Correspondence: hslongrcees@163.com

Abstract: The sustainable restoration of river and lake ecosystems requires advanced wastewater treatment technologies to control nitrogen pollution, a key driver of aquatic degradation. This study explores the physiological responses of anammox granular sludge (AnGS) to varying nitrogen loading rates (NLRs), offering insights into microbial stability under environmental stress. AnGS samples with different particle sizes (<1.0 mm, 1–2 mm, >2 mm) were subjected to NLRs ranging from 0.9 to 3.6 gN/L/d. As the NLR increased, the NO₂[−]-N/NH₄⁺-N consumption ratio rose from 1.0 to 1.2, and the most active particle size shifted to 1–2 mm. Hydroxyapatite (HAP) crystals formed at higher NLRs, enhancing the settling and activity of 1–2 mm AnGS but inhibiting larger granules (>2 mm). Microbial analysis revealed that *Candidatus Brocadia* dominated at high NLRs (10.5%), outperforming *Candidatus Kuenenia* (2.47%). The enrichment of these key genera across granules indicates adaptive microbial migration under loading stress. These findings provide critical operational strategies for sustaining AnGS performance through particle size regulation, contributing to nitrogen control solutions vital for river and lake restoration efforts.

Keywords: anammox; granular; nitrogen removal; particle size; microbial migration

Academic Editor: Jesus Gonzalez-Lopez

Received: 29 April 2025

Revised: 23 May 2025

Accepted: 26 May 2025

Published: 29 May 2025

Citation: Fan, X.; Qian, Y.; Yang, X.; Wang, Y.; Yang, H.; He, S. Multiscale Characterization of Anammox Granules and Microbial Migration Under Variable Nitrogen Loading Rates. *Water* **2025**, *17*, 1653. <https://doi.org/10.3390/w17111653>

Copyright: © 2025 by the authors. Licensee MDPI, Basel, Switzerland. This article is an open access article distributed under the terms and conditions of the Creative Commons Attribution (CC BY) license (<https://creativecommons.org/licenses/by/4.0/>).

1. Introduction

Water pollution remains a significant global challenge, particularly in developing countries [1,2]. Various technologies have been developed to treat wastewater [3,4]. The anammox process is an innovative biological nitrogen removal technology that offers distinct advantages for treating wastewater with high levels of NH₄⁺-N, such as food waste digestate and swine manure digestate [5,6]. However, the growth rate of anammox bacteria (AnAOB) is only 0.0027 h^{−1}, prolonging the startup period of the anammox process and posing a significant obstacle to its widespread engineering application [7].

Achieving effective retention and enrichment of AnAOB is crucial for addressing the low growth rates of AnAOB. The addition of biofilm carriers and the optimization of reactor configurations have been adopted to address this obstacle. A high enrichment of AnAOB was achieved by utilizing a hollow carrier in a gas lift reactor, with a relative abundance of 32.31% [8]. Although the addition of carriers is beneficial for achieving the stability of the anammox process, the long biofilm formation period (up to 210 days) poses an extended risk of AnAOB loss. Membrane bioreactors, which offer efficient biomass retention, are utilized for the effective enrichment of AnAOB, enabling the rapid startup of the anammox process within 63 days [9]. However, membrane bioreactors require high

operating costs [10]. Compared with aerobic sludge, anammox sludge is more likely to secrete extracellular polymeric substances to facilitate the aggregation of anammox flocs into anammox granular sludge (AnGS) [11]. Granules are the primary sludge morphology form of AnAOB [12]. Therefore, it is necessary to evaluate the growth characteristics of the AnGS and the AnGS stability mechanisms.

NLRs can directly affect the physiological characteristics and mechanical strength of AnGS, such as settling velocity, activity, microbial community, and particle size [13,14]. The settling velocity of the AnGS increased from 126 to 198 m/h as NLR was elevated from 1 to 3 gN/L/d [15]. The high settling velocity promotes the maintenance of an adequate AnAOB biomass within the reactor. The AnAOB activity enhanced from 0.38 to 0.8 gN/gVSS/d as the NLR increased from 5 to 50 gN/L/d [16]. As the NLR was elevated from 1.2 to 15.4 gN/L/d, the abundance of *Candidatus Kuenenia* rose from 36.1% to 57.1% [17]. As the NLR elevated from 0.1 to 0.5 g N/L/d, a migration occurred from *Candidatus Kuenenia* to *Candidatus Brocadia* [18]. Additionally, as the influent ratio rose from 1 to 1.25, a migration occurred from *Candidatus Brocadia* to *Candidatus Kuenenia*, with an abundance of 52.3% [17]. Due to the different substrate tolerance conditions of different AnAOB, *Candidatus Kuenenia* is suitable for growing under high NLRs, while *Candidatus Brocadia* is suitable under low NLRs. For wastewater with different total nitrogen concentrations, particle size can be specifically regulated (such as through screening) to achieve maximum nitrogen removal efficiency.

The highest AnAOB activity of 0.17 gN/gVSS/d was achieved with AnGS particles sized from 1.5–2.0 mm when NLR was 0.4 gN/L/d [19]. AnGS particles sized from 2–2.8 mm has been reported to exhibit an optimal SAA of 2.0 gN/gVSS/d at an NLR of 1.5 gN/L/d [15]. At an NLR of 13.6 gN/L/d, AnGS particles sized from 0.5–1 mm exhibited an absolute dominance of 55.7% [20]. AnGS particles sized >4.0 mm were classified as floating granules when the NLR was 44 gN/L/d [21]. These results suggest that the properties of AnGS are closely related to particle size and are influenced by the NLR. However, current studies have concentrated on a single NLR level, and the reported optimal particle sizes for AnGS have not been uniformly established. To address the knowledge gaps, it is essential to investigate the impact of NLRs with wide dimensional fluctuations from low to high on the biochemical and physical properties of sludge with varying particle sizes and to analyze the microbial community relationships from a macro-genetic perspective.

The objectives of this study include the following: (1) to investigate the physicochemical properties of AnGS with different particle sizes under NLR fluctuations ranging from 0.9 to 3.6 gN/L/d, (2) to investigate the microbial community response characteristics of different particle sizes, and (3) to identify the optimal particle size for AnGS.

2. Material and Methods

2.1. Experiment Setup

An 4.5 L expanded granular sludge bed (EGSB) reactor (Shanghai Binyue Plexiglass Production Center, Shanghai, China) was used (Figure 1). The temperature was maintained at 35 ± 1 °C using a heat pump, and a black insulating jacket was applied to prevent the impact of light on the AnGS. A pump was used to control an effluent reflux ratio of 1:1. The effluent from the EGSB reactor is partially treated by a peristaltic pump and reinjected into the bottom of the reactor, where it is mixed with the influent. This design increases the upward flow rate of the reactor, promotes the expansion of the sludge bed, and forms a stable suspended state of granular sludge, thereby expanding the contact area between sludge and wastewater.

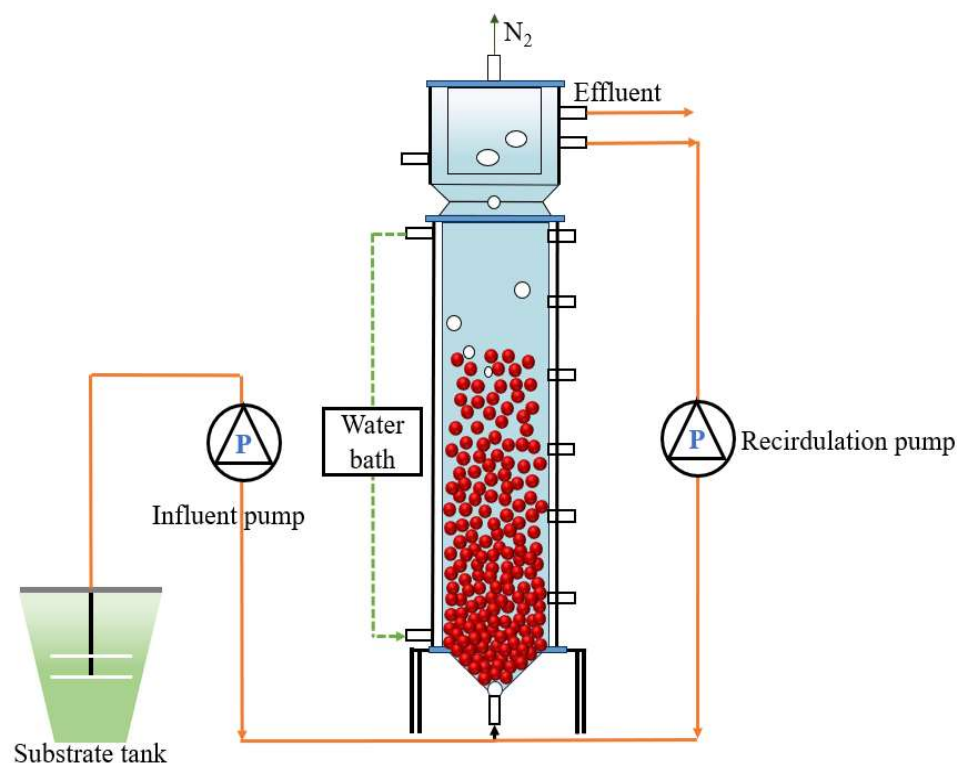


Figure 1. Configuration of the EGSB reactor.

2.2. Reactor Operation

The entire operation was segmented into three phases, based on the influent NO_2^- -N/ NH_4^+ -N ratios and NLRs (Table 1). In Phase I, the TN concentration in influent was 450 mg/L, and the NLR was 0.9 gN/L/d. A previous study reported that the R_s (ΔNO_2^- -N/ ΔNH_4^+ -N) of the anammox process was correlated with the NLR [16]. As NLR was evaluated from 5 to 50 gN/L/d, the R_s was augmented from 1.13 to 1.31. The NLR for Phase I was 0.9 g N/L/d, which is significantly below 5 gN/L/d. Therefore, the NO_2^- -N to NH_4^+ -N ratio in the influent was set to 1. In Phase II, the NO_2^- -N to NH_4^+ -N ratio in the influent was adjusted to 1.15 to prevent substrate inhibition based on the R_s in Phase I, while the TN concentration and NLR were the same as in Phase I. In Phase III, the NLR was increased to 3.6 gN/L/d by shortening the hydraulic retention time (HRT), with a higher influent NO_2^- -N/ NH_4^+ -N ratio of 1.2.

Table 1. The operational conditions and performance of the anammox-EGSB reactor.

Phase	Days (d)	Operation Conditions				Reactor Performance			
		TN_{in} (mg/L)	NO_2^- -in: NH_4^+ -in	HRT (h)	NLR (gN/L/d)	NH_4^+ -eff (mg/L)	NO_2^- -eff (mg/L)	NO_3^- -eff (mg/L)	TNRE (%)
I	1–47	450	1:1	12	0.9	28.98 ± 11.91	10.26 ± 4.71	31.87 ± 7.44	82.69 ± 1.92
II	48–123	450	1.15:1	12	0.9	45.47 ± 16.90	9.11 ± 6.31	53.53 ± 9.37	79.28 ± 0.27
III	124–154	450	1.2:1	3	3.6	16.90 ± 7.976	20.03 ± 13.69	51.79 ± 3.17	83.64 ± 0.59

2.3. Synthetic Wastewater and Inoculum Sludge

The synthetic wastewater was composed of NH_4Cl and NaNO_2 . The detailed composition of the synthetic wastewater was consistent with that reported in a previous study [22].

The AnAOB seed sludge was collected from an EGSB reactor that had been cultured for 3 years. The initial volatile suspended solids (VSS) concentration was 16.7 g/L, with a VSS to suspended solids (SS) ratio of 0.39 [23].

2.4. Properties of AnGS with Different Particle Sizes

The mixed AnGS was filtered into three separate groups, based on particle size: <1.0, 1.0–2.0, and >2.0 mm [24]; the volume proportion of the AnGS was measured in a glass column with a volume of 20 mL. Macroscopic morphological variations of the AnGS were recorded using a mobile phone under identical lighting conditions. The settling velocity was determined in a 1 m hollow glass water column, and 15–20 samples were tested in each group [25]. To test the SAA of the AnGS, at the end of each phase, the AnGS is placed in serum bottles containing substrates, exposed to nitrogen for 10 min, and gas production is regularly measured for analysis [26]. The VSS and SS concentrations of particles with different particle sizes were measured via the APHA method [27]. Each test was set up in parallel to ensure the accuracy of the data. One-way analysis of variance (ANOVA) was conducted using the Statistical Package for the Social Sciences 22.0 to evaluate the significance of the experimental results, with a difference considered statistically significant at $p < 0.05$.

2.5. Analytical and Calculative Methods

The influent and effluent samples from the reactor were filtered using 0.45 μm filters every 2 days. The $\text{NH}_4^+\text{-N}$, $\text{NO}_2^-\text{-N}$, and $\text{NO}_3^-\text{-N}$ were assessed using the standard method [27]. pH was determined using a PHS-25 PH meter (PHS-25, Shanghai Yidian Scientific Instrument Co., Ltd., Shanghai, China). X-ray diffraction (XRD) was applied to measure the AnGS crystals of different sizes. The calculation methods for R_s and R_p are based on the methods used in a previous study [28]. R_s is the ratio of the actual consumption of nitrite nitrogen to ammonia nitrogen. R_p is the ratio of the production of nitrate nitrogen to the consumption of ammonia nitrogen.

2.6. Microbial Community Analysis

At the end of Phase I and III, mixed AnGS and three groups of anammox particulate sludge samples (<1.0, 1.0–2.0, and >2.0 mm) were collected and retained at $-20\text{ }^\circ\text{C}$. Eight sludge samples were analyzed at the Shanghai Majorbio Bioengineering Laboratory. Microbial communities were determined by sequencing using the Illumina MiSeq platform 2.0, and MiSeq sequencing libraries were prepared by two-step tailed PCR, using 515F and 806R as primers.

3. Results and Discussion

3.1. Overall Performance

The performance of the EGSB–anammox reactor is shown in Figure 2. In Phase I, the NLR was 0.9 gN/L/d, EGSB–anammox process exhibited the mean removal efficiency of $\text{NH}_4^+\text{-N}$ and $\text{NO}_2^-\text{-N}$ was $85.74 \pm 5.76\%$ and $95.21 \pm 2.28\%$, respectively (Figure 2c). The mean total nitrogen removal efficiency (TNRE) during the operation phase was $82.69 \pm 1.92\%$, with mean R_s and R_p values of 1.14 ± 0.08 and 0.18 ± 0.04 (Figure 3a,b), respectively. Based on the theoretical stoichiometric equation of anammox process [29], the R_s was 1.32 and R_p was 0.26. At the end of Phase I, the removal efficiency of $\text{NH}_4^+\text{-N}$ reached only 81%, while the $\text{NO}_2^-\text{-N}$ removal efficiency reached 97%. As a result, the R_s and R_p were 1.26 and 0.24, separately (Figure 3a,b). Previous studies have also reported that R_s was 1.14 ± 0.14 when NLR reached 1.0 gN/L/d [30]. The $\text{NO}_2^-\text{-N}$ to $\text{NH}_4^+\text{-N}$ ratio was 1, which conducive to preventing substrate inhibition during the initial period of startup. Then, the AnAOB activity was enhanced and the residual $\text{NH}_4^+\text{-N}$ was the primary factor limiting the improvement of NRE, necessitating adjustments to the influent $\text{NO}_2^-\text{-N}/\text{NH}_4^+\text{-N}$ ratio based on the actual ratio of R_s .

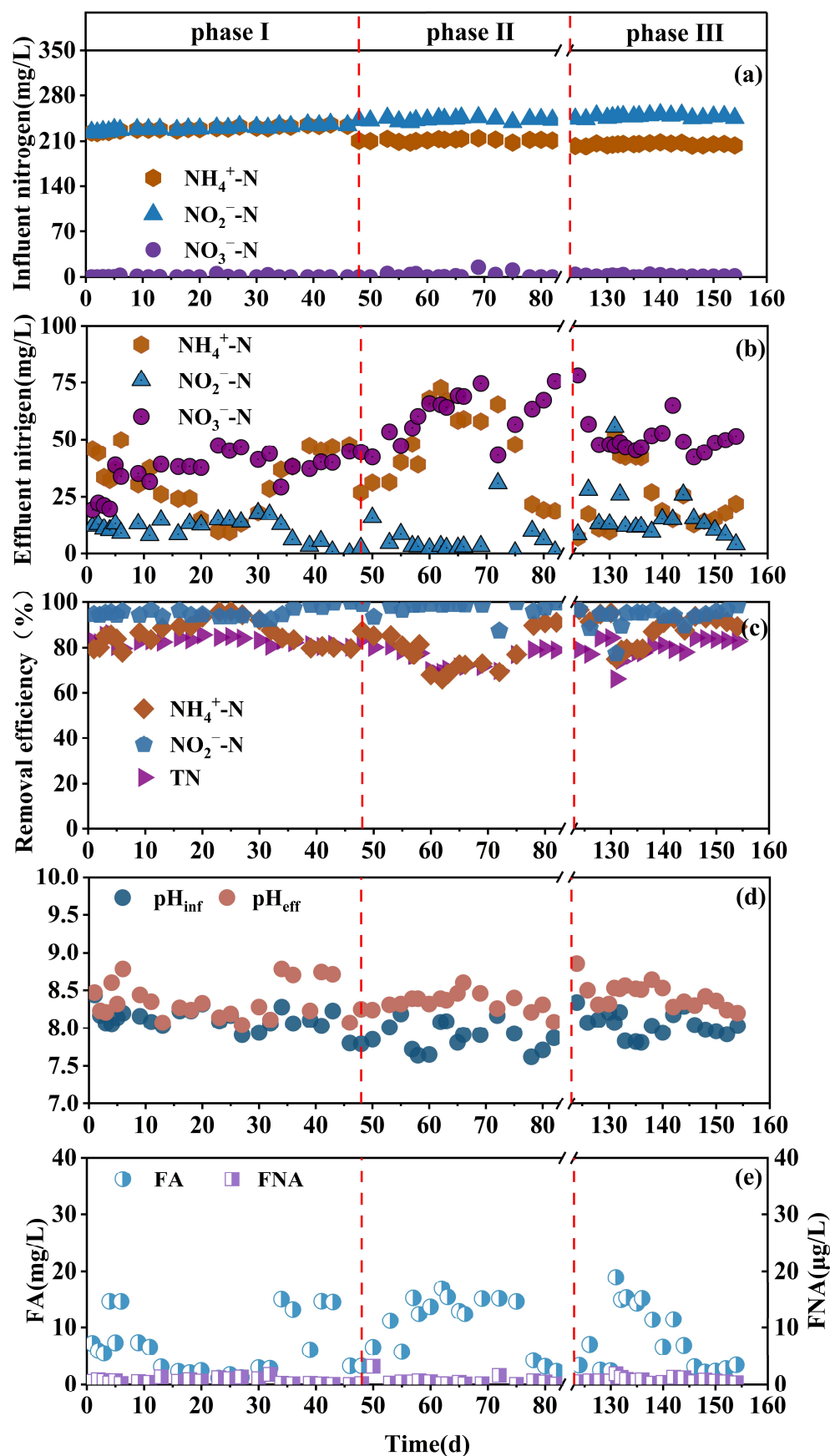


Figure 2. Nitrogen removal performance under various NLRs: (a,b) changes in the concentration of nitrogen species; (c) ammonia, nitrite, and TN removal efficiency; (d) pH in the influent and effluent; (e) FA and FNA contents.

In Phase II, NLR were not changed. The NO_2^- -N to NH_4^+ -N ratio was improved to 1.15. The EGSB–anammox process achieved a mean TNRE of $79.28 \pm 0.27\%$ (Figure 2c), resulting in effluent NO_2^- -N and NH_4^+ -N concentrations of 0.75 mg/L and 16.09 mg/L, respectively (Figure 2b). The R_s was 1.39 ± 0.14 , and R_p was 0.32 ± 0.05 , both exceeding the theoretical values for the anammox reaction. These results indicated that the presence of trace amounts of oxygen in the influent might led to the growth of nitrifying bacteria [31].

In Phase III, a higher NLR was adopted to enhance the anammox activity and inhibit the nitrifying bacteria activity. The TN concentration remained at 450 mg/L while the NO_2^- -N to NH_4^+ -N ratio was improved to 1.2, and the HRT was shortened to 3 h to increase the NLR to 3.6 gN/L/d. The mean TNRE was $83.64 \pm 0.59\%$. The R_s was 1.31 ± 0.03 , and R_p was 0.28 ± 0.04 , approaching the theoretical values.

The R_s is related to the enrichment level of AnAOB and the NLRs. The widely used influent theoretical R_s for anammox was reported in a low NLR condition of 1.0 gN/L/d [32]. The high enrichment level of 67% AnAOB contributed to the high R_s . As the NLR increased from 5 to 50 gN/L/d, the anammox bacteria become enriched, accompanied by the increase in R_s from 1.13 to 1.31 [16]. In this study, the trends of R_s and R_p were consistent with those in previous studies [15,16,30,33,34] (Figure 3c,d). The R_s and R_p corresponding to the NLR in this study were fitted with those from previous studies. Within the NLR range of 0.9–20 gN/L/d, an excellent correlation exists among the results from various studies for R_s (0.9951) and R_p (0.9638). Meanwhile, R_s and R_p increase rapidly within an NLR below 5.0 gN/L/d, subsequently approaching the theoretical values of 1.32 and 0.26, respectively.

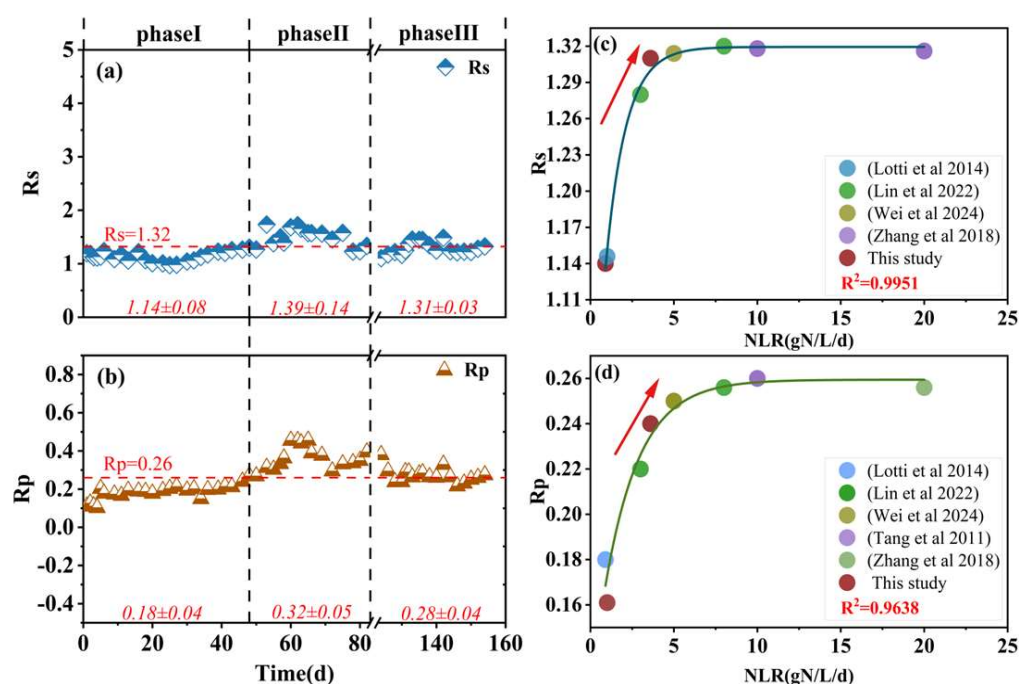


Figure 3. (a) Changes in R_s values; (b) changes in R_p values; (c) relationship between R_s and NLR; (d) relationship between R_p and NLR [15,16,30,33,34].

3.2. Physicochemical Properties of AnGS

3.2.1. Morphology of AnGS at Different Sizes

Figure 4 shows the morphology of the AnGS. In Phase I, the reddish-brown color of AnGS gradually deepened with increasing particle size. The AnGS particles sized <1.0 mm was mainly light red and light brown. AnGS with a 1.0–2.0 mm particle size was pink with irregularly spherical particles. AnGS particles sized >2.0 mm had a more regular spherical shape, and the color was bright red, with a distinct brownish red hue (Figure 4a–c). AnGS

is usually blood red, indicating its activity. The color has been reported to be due to the presence of cytochrome c, and it correlates significantly with the amount and activity of AnAOB [35]. The abundance of anammox can be roughly represented by the degree of redness [36].

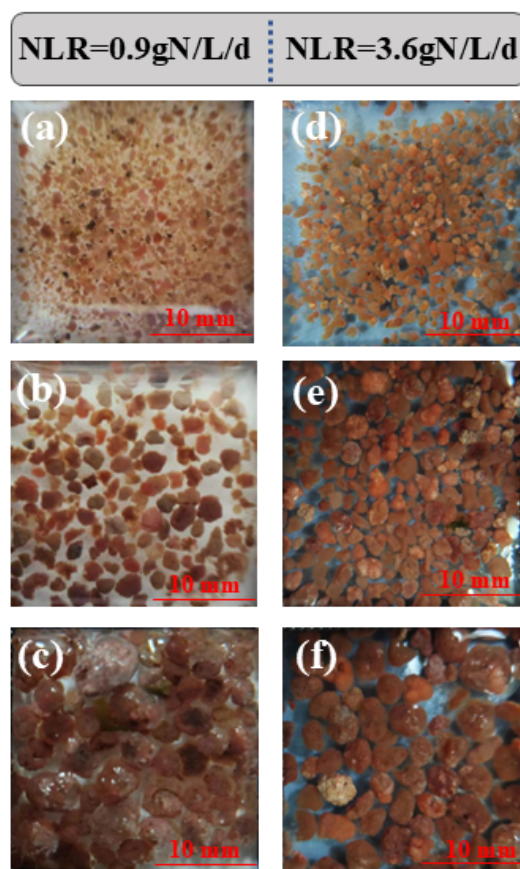


Figure 4. Morphological characteristics of size-fractionated granular sludge: (a–c) images of granular sludge in size categories of <1.0, 1.0–2.0, and >2.0 mm at an NLR of 0.9 gN/L/d; (d–f) images of granular sludge in the same size categories at an NLR of 3.6 gN/L/d.

In Phase III, the color change of the AnGS with increasing particle size is similar to that in Phase I. Notably, the surface of AnGS particles sized 1.0–2.0 mm and >2.0 mm was coated with a thin layer of white inorganic material, which is likely calcium precipitation (Figure 4d–f). Research has indicated that the presence of Ca^{2+} , Fe^{2+} , Mg^{2+} , and Mn^{2+} significantly enhances anammox granulation [37]. Ca^{2+} readily combines with SO_4^{2-} , PO_4^{3-} , and CO_3^{2-} in water to form different types of precipitates. However, these precipitates have been reported to exacerbate mass transfer limitations in mature AnGS [38].

The long-term addition of calcium substrates has been shown to result in the formation of AnGS with a hydroxyapatite (HAP) inorganic core, thereby enhancing their settling properties [39]. However, the precipitation of calcium phosphate can lead to decreased biomass activity [40]. The positive and negative effects of HAP on anammox granules are related to particle size, which exhibited different results among AnGS with different particle sizes. The surface of the particles >2.0 mm exhibited a distribution of compact and irregular white round particles. The whiteness of these particles intensified, and some displayed signs of mineralization. XRD (X-ray diffraction) analysis (Figure S1) indicated that the primary inorganic crystal in sludge particles sized from 1.0–2.0 mm and >2.0 mm was hydroxyapatite (HAP), which is the main mineral present. The HAP crystals were not detected in AnGS particles sized < 1.0 mm. The formation of HAP requires alkalinity provided by anammox, which is closely linked to the activity of the AnGS [41]. Larger

particles indicate higher anammox activity, which promotes the formation of HAP and provides an inorganic core for anammox granules, thereby further facilitating the growth of AnGS [42]. Therefore, HAP crystals are predominantly present in larger particles.

The accumulation of inorganic HAP can provide a core for particle formation, but it may also affect microbial activity [43]. The formation of HAP has been reported to decrease the abundance of AnAOB, thereby obstructing substrate mass transfer and ultimately leading to bacterial death [44]. In this study, the effects of HAP on AnGS with different particle sizes will be analyzed from several aspects, including settling property, activity, and microbial community structure.

3.2.2. Percentage of Granular Sludge

In Phase I, the particle sizes of anammox sludge were primarily concentrated in the <1.0 mm range, which accounted for 42.79%. Meanwhile, AnGS particles sized 1.0–2.0 mm and >2.0 mm accounted for 32.68% and 24.51%, respectively (Figure 5a). In Phase III, AnGS particles sized 1.0–2.0 mm were the most abundant, with a percentage of 57.32%. Conversely, AnGS particles sized <1.0 mm accounted for 24.57%. The proportion of AnGS particles sized >2.0 mm remained relatively constant. The results suggest that as the NLR increases, the dominant particle size of AnGS shifts from <1.0 mm to 1.0–2.0 mm. This shift may result from the migration of anammox particles among different particle sizes. Under higher NLR conditions, AnGS is likely to release more extracellular polymeric substances to promote granule formation [11]. Research has indicated that the ideal particle size shifts from 0.6–1.6 mm to 1.6–2.5 mm as the NLR increases [45]. As the NLR increased from 18.7 to 37.9 gN/L/d, the proportion of AnGS particles sized 0.5–1.0 mm increased from 46% to 58% [20]. Under NLR impacts, the biofilm surrounding the AnAOB and the central core may detach, leading to a decrease in the size of immature granular sludge particles, which then adhere to each other to form larger particles [46].

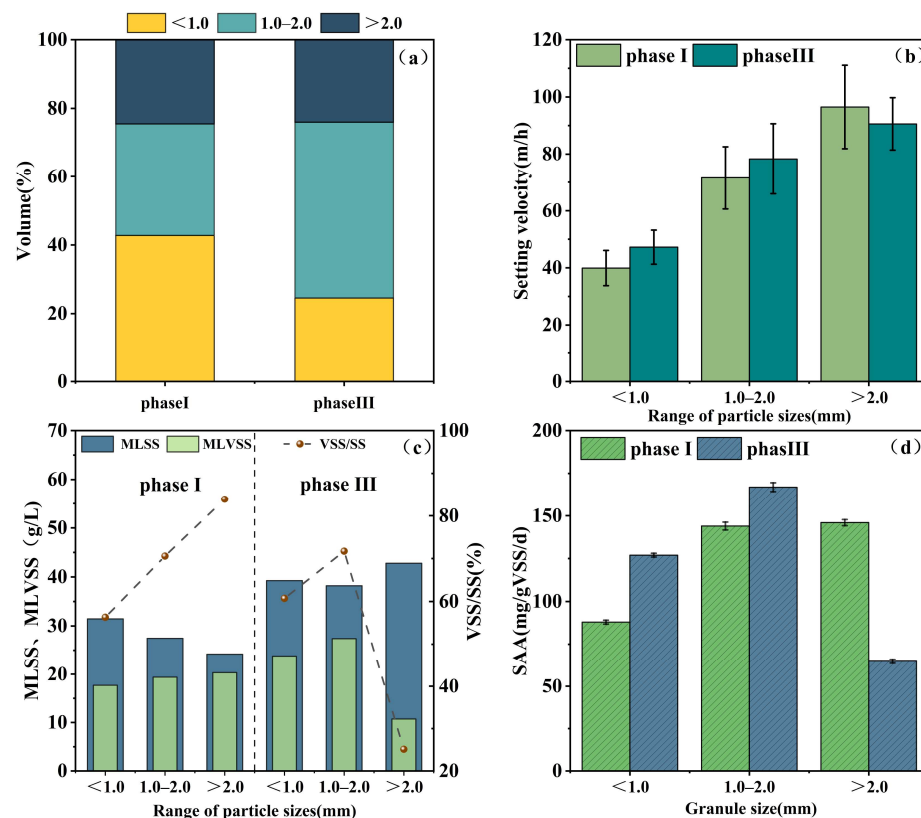


Figure 5. Percentage by volume (a) and settling velocity (b) of the sludge; sludge characteristics, where sludge concentrations are measured in (c); (d) SAA analysis of the granular sludge.

3.2.3. Sludge Settling Velocity

The improved settling ability of the sludge helps reduce biomass loss, thereby improving the retention rate of AnAOB [47]. In Phase I, the settling velocity of particles increased with particle size (Figure 5b). The average settling velocities of AnGS with particle sizes of <1.0 mm, 1–2 mm, and >2.0 mm were 39.92 ± 6.15 m/h, 71.58 ± 10.97 m/h, and 96.49 ± 14.62 m/h, respectively. In Phase III, the average settling velocities of AnGS with particle sizes of <1.0 mm and 1.0–2.0 mm were 47.24 ± 5.98 m/h and 78.29 ± 12.34 m/h, respectively. The accumulation of inorganic materials and the formation of hydroxyapatite (HAP) contributed to the improved settling performance. The formation of HAP was reported to increase the settling rate of AnGS particles sized >2.8 mm from 130 m/h to 210 m/h [48]. HAP plays a beneficial role in the retention of AnGS. However, the settling velocity of AnGS particles sized >2.0 mm was 90.56 ± 9.18 m/h. Research has shown that the accumulation of HAP crystals in mature AnGS hinders mass transfer, thereby impeding the release of nitrogen gas and resulting in a decrease in settling velocity [49].

An increase in the percentage of inorganic content in AnGS can enhance the settling velocity of the AnGS [24]. In Phase I, the VSS/SS ratios of AnGS with particle sizes of <1.0, 1.0–2.0, and >2.0 mm were 0.56, 0.71, and 0.84, respectively (Figure 5c). Under low NLR conditions, there were few inorganic components in the large particles of AnGS. The same phenomenon was also observed in an upflow anaerobic sludge blanket; as the particle size increased, the VSS/SS ratio gradually increased from 0.32 to 0.88 when the NLR reached 1.05 gN/L/d [50]. However, another study found that the VSS/SS ratios for AnGS particles sized 0.75, 1.28, 1.83, and 2.67 mm were 0.51, 0.50, 0.45, and 0.40, respectively [19]. In Phase III, the VSS/SS ratios of AnGS with a particle size of <1.0 mm and 1–2 mm were 0.61 and 0.71, respectively (Figure 5c). Notably, the VSS/SS ratio of AnGS particles sized >2.0 mm was 0.25. There were more inorganic components and less biomass in large particles. A previous study reported that anammox particles sized >2.0 mm, with a VSS/SS of 0.15, exhibit high surface inorganic content, leading to impeded mass transfer when NLR was 2.8 gN/L/d [51]. It was reported that anammox biomass decreased in response to the HAP formation [44]. In this study, HAP was identified as the predominant crystal in AnGS particles >2.0 mm, promoting biomass retention. However, the accumulation of HAP also impacts the activity of the AnGS, a topic discussed in Section 3.2.4.

3.2.4. Specific Anammox Activity

SAA is a crucial factor for evaluating the nitrogen removal performance of AnGS (Figure 5d). In Phase I, the SAA results were 88 ± 1.85 , 144 ± 2.3 , and 146 ± 1.8 mg N/g VSS/d for AnGS particles sized <1.0 mm, 1.0–2.0 mm, and >2.0 mm, respectively. The optimal particle size for AnGS was >2.0 mm. In Phase III, the SAA of AnGS particles sized <1.0 mm was 127 ± 1.1 mg N/g VSS/d, and that of particles sized 1–2 mm was 167 ± 2.6 mg N/g VSS/d. However, the SAA of AnGS particles sized >2.0 mm was 64.95 ± 1.2 mg N/g VSS/d. The trend in SAA across different particle sizes in Phase I and III aligned with the trend of MLVSS ($p < 0.01$), indicating that variations in SAA related to particle size can be attributed to biomass content. A similar trend was observed on AnGS particles sized 2.0–2.8 mm as the NLR raised to 3.0 gN/L/d [15]. When NLR was 3.6 gN/L/d, the optimal particle size was 1.0–2.0 mm. HAP was detected in large AnGS particles (>1.0 mm). The activity and proportion of AnGS with a particle size of 1.0–2.0 mm both increased, indicating that HAP is beneficial for AnGS. However, the accumulation of HAP in granular sludge sized >2.0 mm caused a reduction in biomass and AnAOB substrate starvation, leading to a decrease in AnAOB activity.

3.3. Microbial Community

3.3.1. Taxonomic Results

At the phylum level of mixed AnGS, the microorganisms mainly include *Planantomycetota*, *Proteobacteria*, *Chloroflexi*, *Bacteroidota*, and *Acidobacteriota*, which are widely present in Phase I and III, with a total abundance of 82.33–92.55% (Figure 6a).

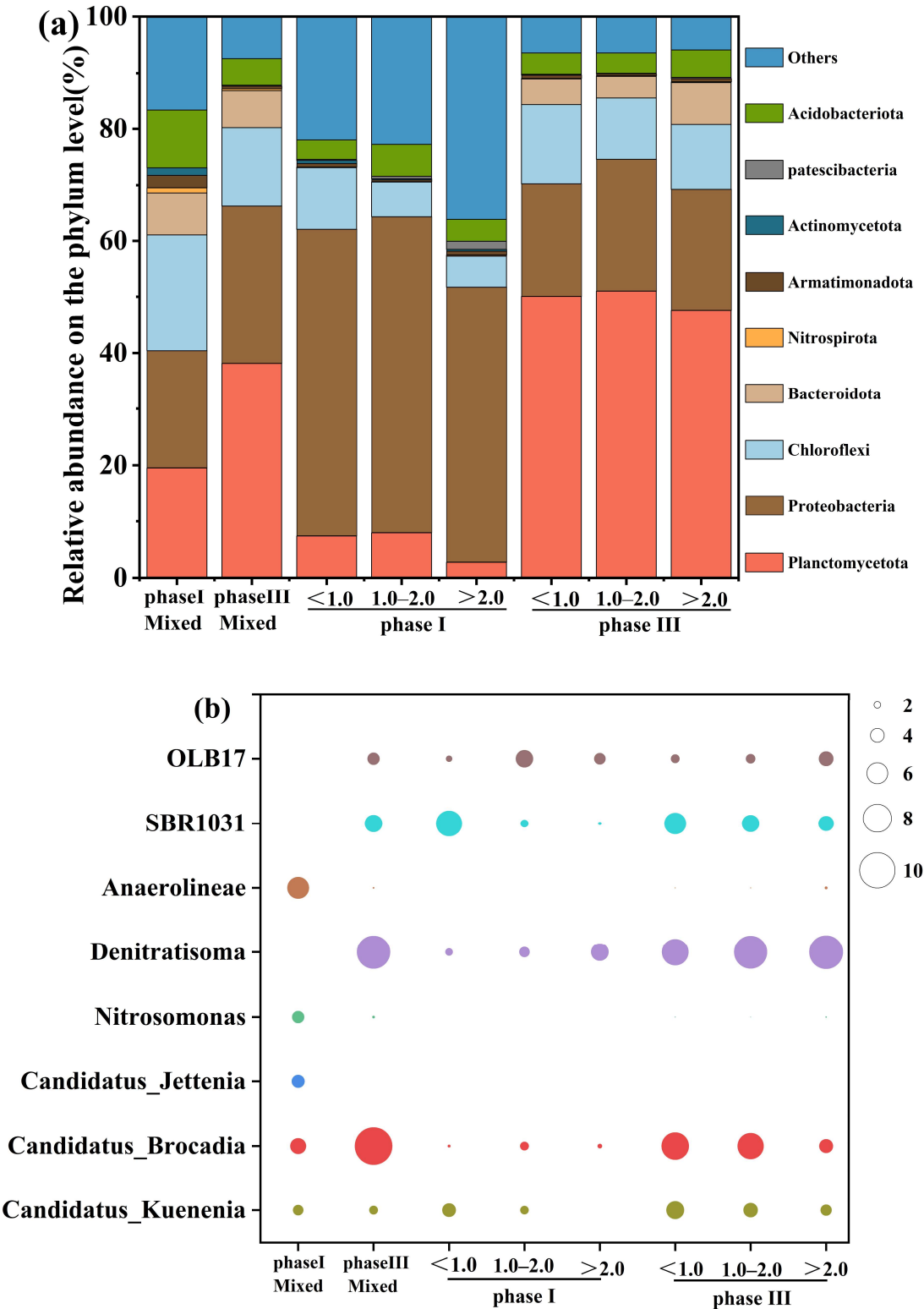


Figure 6. Relative abundance of predominant microbes in the mixed sludge and granular sludge with three different particle sizes at the phylum level (a) and genus level (b). An abundance of <0.5% is categorized as “others”.

Significant community differences were observed at the phylum level of AnGS with different particle sizes. The abundance of phylum *Plananctomycetota* increased significantly with particle size from 7.38%, 7.96%, and 2.74% to 49.88%, 50.97%, and 47.33%, respectively. Increasing the NLR is beneficial for the growth of AnAOB. Conversely, the abundance of phylum *Proteobacteria* decreased from 54.65%, 56.31%, and 46.09% to 20.09%, 23.39%, and 21.56%, respectively. The highest abundance of phylum *Plananctomycetota* and phylum *Proteobacteria* was exhibited in AnGS particles sized 1.0–2.0 mm. *Chloroflexi* was evenly distributed among the different particle sizes (14.02%, 10.85%, 11.48%). The phylum *Chloroflexi* has been reported to enhance the structure of the AnAOB communities and promote coordinated denitrification among various bacteria in the system [43]. The abundance of phylum *Bacteroidetes* increased to 4.67%, 3.94%, and 7.52%, respectively. Bacteroidetes are critical for the dispersion of AnAOB, and their increased abundance could be linked to sludge pelleting [4].

At the genus level of mixed AnGS (Figure 6b), the AnAOB identified in Phase I and Phase III were mainly *Candidatus Brocadia*, *Candidatus Kuenenia*, and *Candidatus Jettenia*. For mixed sludge, the abundance of *Candidatus Brocadia* increased prominently from 4.47% to 10.51%. *Candidatus Brocadia* was reported to follow a growth rate (r) strategy, better suited for high NLR environments [52]. However, the abundance of *Candidatus Jettenia* was not detected in Phase III. This may be due to the weaker substrate competitiveness of *Candidatus Jettenia* under higher NLR [53]. Research has shown that under low NLR, *Candidatus Jettenia* competes more effectively for nitrite than does *Candidatus Brocadia*, while under high NLR, *Candidatus Brocadia* outcompetes *Candidatus Jettenia* for substrates, resulting in a decrease in the abundance of *Candidatus Jettenia* [54]. *Candidatus Kuenenia* and *Candidatus Brocadia* were detected in particles of different sizes. However, under a high influent substrate ratio, the abundance of *Candidatus Brocadia* in different particle sizes was significantly increased (10.5%). This is because adjusting the influent substrate ratio resulted in a decrease in effluent TN concentration, making it more suitable for the growth of *Candidatus Brocadia*, with low substrate tolerance. Additionally, *Nitrosomonas* decreased from 3.46% to 0.74%. The relative abundance of denitrifying organisms (*Denitratisoma*) increased to 9.35%, which may be attributed to the death of certain microorganisms that were not well-suited to the high NLR condition, thereby providing a carbon source for the thriving denitrifying bacteria [55].

At the genus level of AnGS with different particle sizes, the abundance of *Candidatus Kuenenia* distinctly increased from 3.84%, 2.43%, and 0.09% to 4.99%, 4.07%, and 3.17%, respectively. *Candidatus Kuenenia* was evenly distributed among the different particle sizes. *Candidatus Brocadia* was enriched prominently in AnGS particles sized <1.0 mm (7.71%) and 1–2 mm (7.36%). Additionally, the lowest anammox abundance (7.08%) was detected in AnGS particles sized >2 mm, indicating that anammox granules of this size are not beneficial for AnAOB growth. The abundance of denitrifying bacteria significantly increased in all three particle sizes, with the highest abundance observed in particles >2.0 mm, which indicates that a higher NLR is more suitable for the co-denitrification of multiple anammox species.

The aggregation of microbial communities across different phases was analyzed using principal component analysis (PCA) (Figure 7). The results indicated that the three particle sizes of AnGS in Phase I were dispersed in distant areas, while they were clustered more closely in Phase III, reflecting the high correlation and complex functional relationships within the community. Increasing NLR may help improve the biological aggregation of the anammox system.

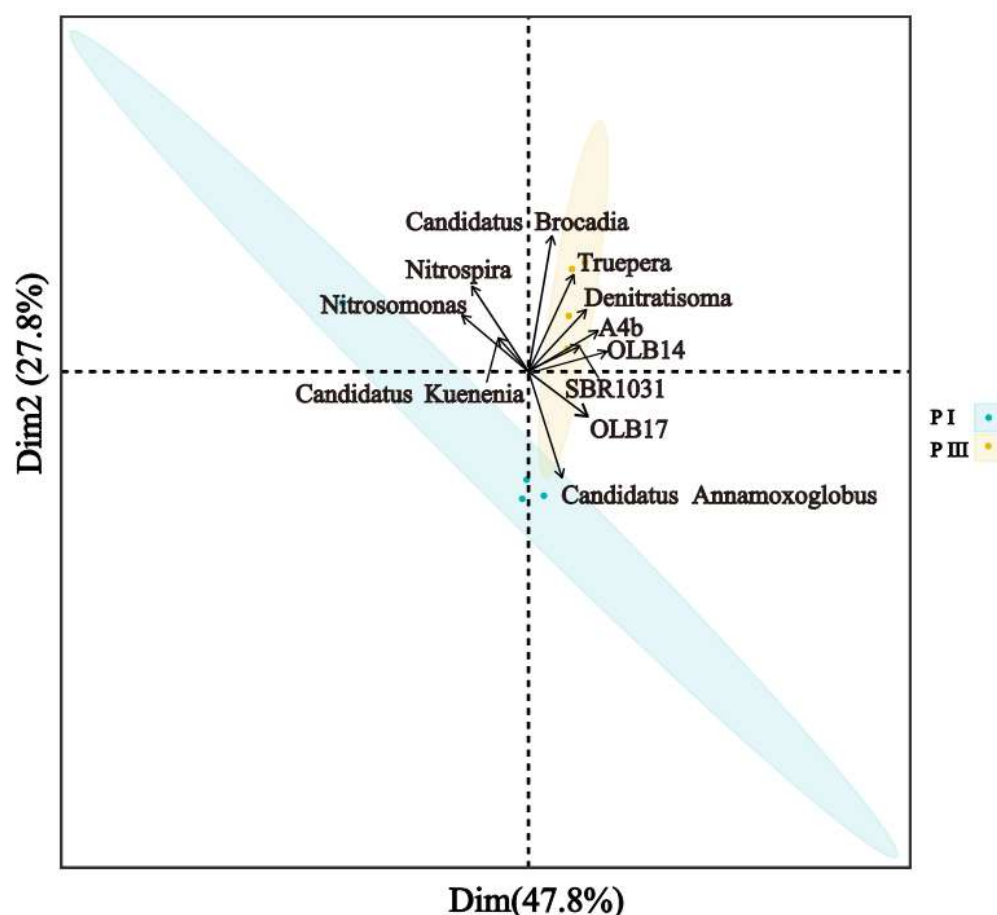


Figure 7. The PCA analysis of AnGS with varying particle sizes at the genetic level. P I: Phase I; P III: Phase III.

3.3.2. Interrelationships Between Major Microbial Communities

The interconnections among dominant microbial genera were analyzed using Pearson's correlation analysis (Figure 8a,b). In Phase I, *Candidatus Kuenenia* demonstrated a negative association with *Candidatus Brocadia* ($R = -0.15$, $p < 0.05$), indicating a weak competitive relationship. Additionally, *Candidatus Kuenenia* displayed a strong positive correlation with *SBR1031* ($R = 0.89$, $p < 0.05$) but exhibited negative correlations with *Denitratisoma* ($R = -1$ and -0.33 , $p < 0.05$) and *OLB17* ($R = -1$ and -0.33 , $p < 0.05$). *Candidatus Kuenenia* and *SBR1031* exhibited a synergistic coexistence relationship. *Denitratisoma* was most abundant in >2.0 mm granular sludge, where it competed for substrates with *Candidatus Kuenenia*, resulting in a lower *Candidatus Kuenenia* abundance. Conversely, *Candidatus Brocadia* was positively correlated with *OLB17* ($R = 0.98$, $p < 0.05$), exhibiting the highest abundance in 1.0–2.0 mm granular sludge. *OLB17* has been shown to promote interdependence between *Candidatus Brocadia* and other AnAOB, reflecting the complex dynamics of microbial communities [56].

In Phase III, *Candidatus Kuenenia* was positively correlated with *Candidatus Brocadia* ($R = 0.90$, $p < 0.05$). The abundance of AnAOB is the lowest in granular sludge with a particle size of >2.0 mm. *Candidatus Kuenenia* and *Candidatus Brocadia* were negatively correlated with *Denitratisoma* ($R = -0.91$ and -0.64 , $p < 0.05$), which indicates that under a higher NLR, denitrifying bacteria are more likely to grow. Due to high NLR, bacteria that are not adapted to the environment will die, providing a carbon source for denitrifying bacteria.

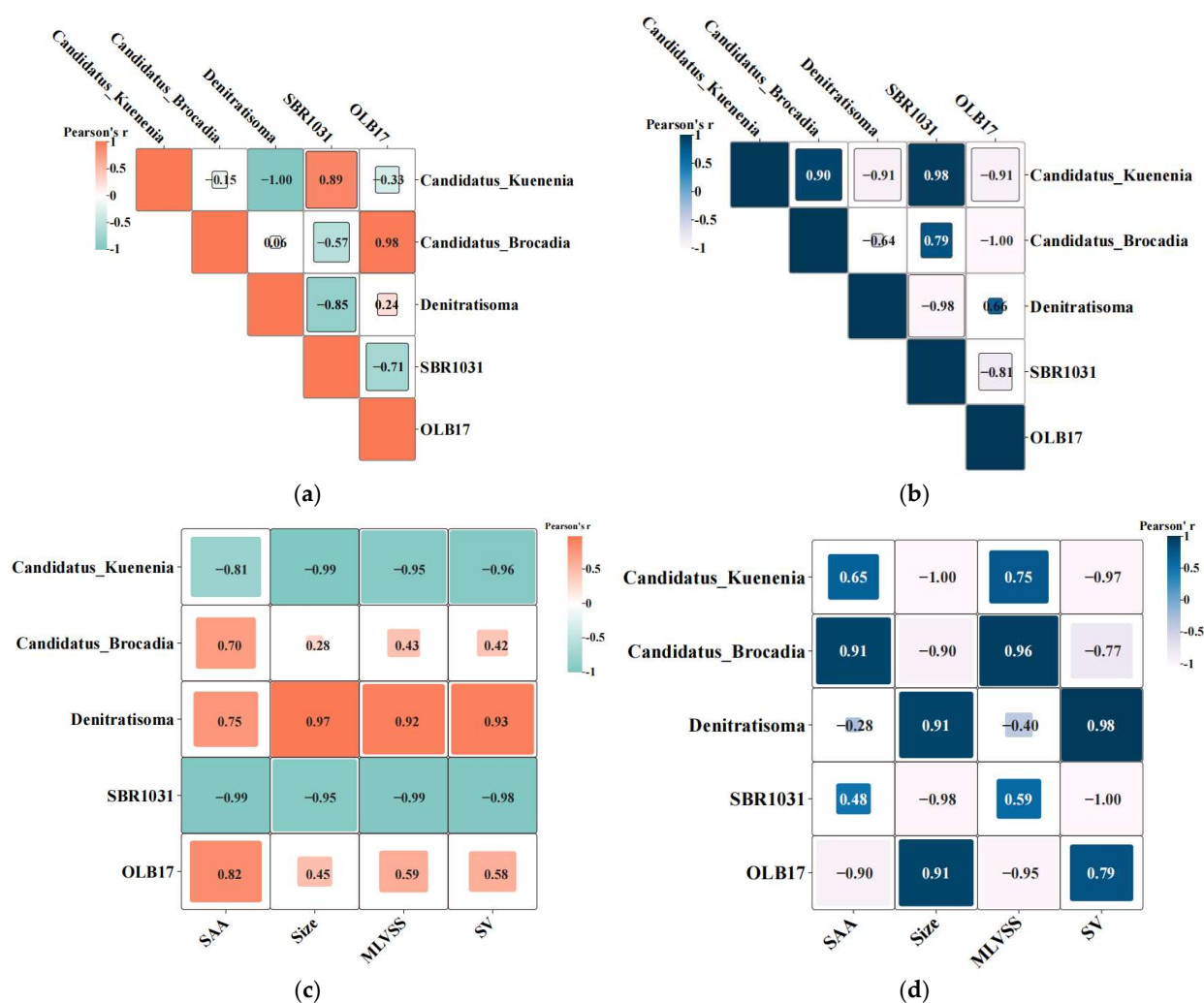


Figure 8. Pearson's correlation analysis was conducted to examine the primary microbial communities at the genus level in Phase I (a) and Phase III (b), as well as to assess the relationships between the dominant genera and environmental factors in Phase I (c) and Phase III (d).

3.3.3. Pearson's Correlation Analysis Between Genera and Environmental Factors

Pearson's correlation analysis between the main genera and environmental factors (Figure 8c,d). In Phase I, the SAA was positively correlated with *Candidatus Brocadia* ($R = 0.7, p < 0.05$) and *Denitratisoma* ($R = 0.75, p < 0.05$), indicating a synergistic nitrogen removal process facilitated by AnAOB and denitrifying bacteria. The collaborative action of functional microorganisms, including AnAOB, denitrifying, and anaerobic digesting bacteria, has been widely recognized as an essential factor in improving nitrogen removal [9]. *Denitratisoma* showed positive correlations with specific anammox activity (SAA), particle size, volatile suspended solids (VSS), and settling velocity (SV). *Candidatus Kuenenia* and *OLB17* were negatively correlated with all four parameters. In Phase III, *Candidatus Kuenenia*, *Candidatus Brocadia*, and *SBR1031* emerged as the primary bacteria positively correlated with SAA. Particle size exhibited positive correlations with *Denitratisoma* and *OLB17* ($R = 0.91, p < 0.05$), suggesting that their presence may also enhance the settlement of granular sludge.

4. Conclusions

This study evaluated the granular characteristics and microbial community migration of AnGS particles under varying NLRs. As the NLR was elevated from 0.9 gN/L/d to 3.6 gN/L/d, the ratio $\text{NO}_2^- \text{-N}$ to $\text{NH}_4^+ \text{-N}$ influent increased from 1 to 1.2, and the TNRE

increased from 82.69% to 83.64%. The optimal particle size for AnGS was >2.0 mm when the NLR was 0.9 gN/L/d, whereas the optimal particle size was 1.0–2.0 mm at an NLR of 3.6 gN/L/d. HAP formed in AnGS particles sized > 2.0 mm and adversely affected the activity. The primary genera of anammox shifted from *Candidatus Kuenenia*, *Candidatus Brocadia*, and *Candidatus Jettenia* to *Candidatus Kuenenia* and *Candidatus Brocadia*. *Candidatus Brocadia* occupied a dominant ecological niche across different particle sizes. These findings offer valuable operational strategies for maintaining a robust AnGS performance through targeted particle size regulation, contributing to an enhanced nitrogen removal process critical for sustainable river and lake restoration.

Supplementary Materials: The following Supporting Information can be downloaded at: <https://www.mdpi.com/article/10.3390/w17111653/s1>, Figure S1: The X-ray diffraction analysis of granular sludge sized >2.0 mm (a), 1.0–2.0 mm (b), and <1.0 mm (c).

Author Contributions: Data curation, X.F. and H.Y. formal analysis, Y.W. Funding acquisition, S.H. Investigation, X.F. Software, Y.Q. Validation, X.Y. Writing—original draft, X.F. Writing—review and editing, S.H. All authors have read and agreed to the published version of the manuscript.

Funding: This study was supported by the Open Project Program of State Key Laboratory of Petroleum Pollution on Control (PPC2019011).

Data Availability Statement: The original contributions presented in this study are included in the article/Supplementary Material. Further inquiries can be directed to the corresponding author.

Conflicts of Interest: The authors declare no conflict of interest.

Nomenclature

VSS	volatile suspended solids
SS	suspended solids
HRT	hydraulic retention time
TN	total nitrogen
Anammox	anaerobic ammonium oxidation
AnAOB	anammox bacteria
NLR	nitrogen loading rate
HAP	hydroxyapatite
SAA	specific anammox activity
TNRE	total nitrogen removal efficiency
PCA	principal component analysis
SV	settling velocity

References

1. Yang, H. Let the Olympics serve as warning for water quality. *Nat. Water* **2024**, *2*, 912. [CrossRef]
2. Yang, H.; Xie, P.; Ni, L.; Flower, R.J. Pollution in the Yangtze. *Science* **2012**, *337*, 410. [CrossRef] [PubMed]
3. Kong, F.; Wang, W.; Wang, X.; Yang, H.; Tang, J.; Li, Y.; Shi, J.; Wang, S. Performance and mechanism of nano Fe-Al bimetallic oxide enhanced constructed wetlands for the treatment of Cr(VI)-contaminated wastewater. *Environ. Res.* **2025**, *271*, 121154. [CrossRef]
4. Li, J.; Peng, Y.; Zhang, Q.; Li, X.; Yang, S.; Li, S.; Zhang, L. Rapid enrichment of anammox bacteria linked to floc aggregates in a single-stage partial nitrification-anammox process: Providing the initial carrier and anaerobic microenvironment. *Water Res.* **2021**, *191*, 116807. [CrossRef]
5. Tan, J.; Ye, M.; Lin, C.; Yu, B.; Li, Y.Y.; Liu, J. Assigning strategic COD flow to enhance denitrification coupled with anaerobic digestion and anammox for systematic upgradation of advanced nitrogen removal from food waste digestate. *Chem. Eng. J.* **2024**, *493*, 152740. [CrossRef]
6. Wu, Y.J.; Weng, T.Y.; Yeh, T.Y.; Chou, P.J.; Whang, L.M. Nitrogen removal strategy for real swine wastewater by combining partial nitrification-denitrification process with anammox. *Chemosphere* **2024**, *364*, 143116. [CrossRef]

7. Kumwimba, M.N.; Lotti, T.; Şenel, E.; Li, X.; Suanon, F. Anammox-based processes: How far have we come and what work remains? A review by bibliometric analysis. *Chemosphere* **2020**, *238*, 124627. [\[CrossRef\]](#)
8. Qian, Y.; Guo, Y.; Shen, J.; Qin, Y.; Li, Y.Y. Biofilm growth characterization and treatment performance in a single stage partial nitrification/anammox process with a biofilm carrier. *Water Res.* **2022**, *217*, 118437. [\[CrossRef\]](#)
9. Zhang, Q.; Zhang, J.; Zhao, L.; Liu, W.; Chen, L.; Cai, T.; Ji, X.M. Microbial dynamics reveal the adaptation strategies of ecological niche in distinct anammox consortia under mainstream conditions. *Environ. Res.* **2022**, *215*, 114318. [\[CrossRef\]](#)
10. Rong, C.; Song, Y.; Yan, W.; Zhang, T.; Li, Y.Y. Anaerobic membrane bioreactor and Anammox in municipal wastewater treatment: Mainstream versus side-stream, challenges, and prospects. *Renew. Sust. Energ. Rev.* **2025**, *210*, 115154. [\[CrossRef\]](#)
11. Ni, S.Q.; Sun, N.; Yang, H.; Zhang, J.; Ngo, H.H. Distribution of extracellular polymeric substances in anammox granules and their important roles during anammox granulation. *Biochem. Eng. J.* **2015**, *101*, 126–133. [\[CrossRef\]](#)
12. Lin, X.; Wang, Y. Microstructure of anammox granules and mechanisms underlying their intensity revealed by microscopic inspection and rheometry. *Water Res.* **2017**, *120*, 22–31. [\[CrossRef\]](#) [\[PubMed\]](#)
13. Wang, X.; Yang, H.; Su, Y.; Liu, X. Characteristics and mechanism of anammox granular sludge with different granule size in high load and low rising velocity sewage treatment. *Bioresour. Technol.* **2020**, *312*, 123608. [\[CrossRef\]](#) [\[PubMed\]](#)
14. Fu, H.M.; Jiang, X.W.; Sun, C.P.; Li, S.J.; Weng, X.; Peng, M.W.; Shen, Y. Exploring the physical disruptions of anammox granular sludge under propylene glycol stress: Implications for nitrogen removal long-term stability. *J. Water Process Eng.* **2025**, *71*, 107405. [\[CrossRef\]](#)
15. Wei, L.; Hu, Y.; Xue, Y.; Tian, W.; Xue, Y.; Chen, R. Granular sludge characterization and microbial response in a hydroxyapatite (HAP)-anammox coupled process at different nitrogen loading rates. *J. Water Process Eng.* **2024**, *64*, 105582. [\[CrossRef\]](#)
16. Zhang, Y.; Ma, H.; Chen, R.; Niu, Q.; Li, Y.Y. Stoichiometric variation and loading capacity of a high-loading anammox attached film expanded bed (AAEEB) reactor. *Bioresour. Technol.* **2018**, *253*, 130–140. [\[CrossRef\]](#)
17. Lin, L.; Zhao, W.; Cui, S.; Song, Y.; Zhang, Y.; Li, Y.Y. Kuenenia-enriched hydroxyapatite granules enable stable high-rate nitrogen removal of high strength food waste permeate in an EGSB-anammox system: Insights into granule performance and process scalability. *J. Water Process Eng.* **2025**, *72*, 107642. [\[CrossRef\]](#)
18. Liu, L.; Ji, M.; Wang, F. Microbial community shift and functional genes in response to nitrogen loading variations in an anammox biofilm reactor. *J. Int. Biodeterior. Biodegrad.* **2020**, *153*, 105023. [\[CrossRef\]](#)
19. Chen, C.; Jiang, Y.; Zou, X.; Guo, M.; Liu, H.; Cui, M.; Zhang, T.C. Insight into the influence of particle sizes on characteristics and microbial community in the anammox granular sludge. *J. Water Process Eng.* **2021**, *39*, 101883. [\[CrossRef\]](#)
20. Wang, Y.; Meng, Y.; Luan, F. High loading start-Up and rapid loading increase of an Anammox UASB reactor generate superior anammox granules. *Water Air Soil Poll.* **2023**, *234*, 166. [\[CrossRef\]](#)
21. Lu, H.; Ji, Q.; Ding, S.; Zheng, P. The morphological and settling properties of ANAMMOX granular sludge in high-rate reactors. *Bioresour. Technol.* **2013**, *143*, 592–597. [\[CrossRef\]](#) [\[PubMed\]](#)
22. Guo, Y.; Li, Y.Y. Hydroxyapatite crystallization-based phosphorus recovery coupling with the nitrogen removal through partial nitrification/anammox in a single reactor. *Water Res.* **2020**, *187*, 116444. [\[CrossRef\]](#) [\[PubMed\]](#)
23. Qian, Y.; Zhang, W.; Wang, Y.; Yang, X.; Guo, J.; He, S. Insights into the influence of organic and salinity on the two-stage partial nitrification/anammox process in treating food waste digestate. *Environ. Technol.* **2024**, *46*, 2469–2484. [\[CrossRef\]](#)
24. Lin, L.; Ishida, K.; Zhang, Y.; Usui, N.; Miyake, A.; Abe, N.; Li, Y.Y. Improving the biomass retention and system stability of the anammox EGSB reactor by adding a calcium silicate hydrate functional material. *Sci. Total Environ.* **2023**, *857*, 159719. [\[CrossRef\]](#)
25. An, P.; Xu, X.; Yang, F.; Li, Z. Comparison of the characteristics of anammox granules of different sizes. *Biotechnol. Bioproc. Eng.* **2013**, *18*, 446–454. [\[CrossRef\]](#)
26. Zhang, Y.; Niu, Q.; Ma, H.; He, S.; Kubota, K.; Li, Y.Y. Long-term operation performance and variation of substrate tolerance ability in an anammox attached film expanded bed (AAFEb) reactor. *Bioresour. Technol.* **2016**, *211*, 31–40. [\[CrossRef\]](#)
27. APHA. *Standard Methods for the Examination of Water and Wastewater*; American Water Works Association and Water Environment Federation: Washington, DC, USA, 2005.
28. Liu, Y.; Zhu, Y.; Deng, J.; Yan, B.; Zhan, J.; Wei, Y.; Gui, S. In Situ Enrichment of Anammox Bacteria from Pig Farm Anoxic Sludge Through Co-Cultivation with a Quorum-Sensing Functional Strain *Pseudomonas aeruginosa*. *Fermentation* **2024**, *10*, 548. [\[CrossRef\]](#)
29. Van de Graaf, A.A.; de Bruijn, P.; Robertson, L.A.; Jetten, M.S.; Kuenen, J.G. Autotrophic growth of anaerobic ammonium-oxidizing micro-organisms in a fluidized bed reactor. *Microbiology* **1996**, *142*, 2187–2196. [\[CrossRef\]](#)
30. Lin, L.; Luo, Z.; Ishida, K.; Urasaki, K.; Kubota, K.; Li, Y.Y. Fast formation of anammox granules using a nitrification-denitrification sludge and transformation of microbial community. *Water Res.* **2022**, *221*, 118751. [\[CrossRef\]](#)
31. Slikers, A.O.; Haaijjer, S.C.; Stafsnes, M.H.; Kuenen, J.G.; Jetten, M.S. Competition and coexistence of aerobic ammonium- and nitrite-oxidizing bacteria at low oxygen concentrations. *Appl. Microbiol. Biot.* **2005**, *68*, 808–817. [\[CrossRef\]](#)
32. Strous, M.; Heijnen, J.J.; Kuenen, J.G.; Jetten, M.S. The sequencing batch reactor as a powerful tool for the study of slowly growing anaerobic ammonium-oxidizing microorganisms. *Appl. Microbiol. Biot.* **1998**, *50*, 589–596. [\[CrossRef\]](#)

33. Tang, C.J.; Zheng, P.; Wang, C.H.; Mahmood, Q.; Zhang, J.Q.; Chen, X.G.; Chen, J.W. Performance of high-loaded ANAMMOX UASB reactors containing granular sludge. *Water Res.* **2011**, *45*, 135–144. [\[CrossRef\]](#) [\[PubMed\]](#)
34. Lotti, T.; Kleerebezem, R.; Lubello, C.; van Loosdrecht, M.C. Physiological and kinetic characterization of a suspended cell anammox culture. *Water Res.* **2014**, *60*, 1–14. [\[CrossRef\]](#)
35. Kartal, B.; Keltjens, J.T. Anammox biochemistry: A tale of heme c proteins. *Trends Biochem. Sci.* **2016**, *41*, 998–1011. [\[CrossRef\]](#)
36. Kang, D.; Li, Y.; Xu, D.; Li, W.; Li, W.; Ding, A.; Zheng, P. Deciphering correlation between chromaticity and activity of anammox sludge. *Water Res.* **2020**, *185*, 116184. [\[CrossRef\]](#)
37. Yu, H.Q.; Tay, J.H.; Fang, H.H. The roles of calcium in sludge granulation during UASB reactor start-up. *Water Res.* **2001**, *35*, 1052–1060. [\[CrossRef\]](#)
38. Jiang, H.L.; Tay, J.H.; Liu, Y.; Tiong-Lee Tay, S. Ca²⁺ augmentation for enhancement of aerobically grown microbial granules in sludge blanket reactors. *Biotechnol. Lett.* **2003**, *25*, 95–99. [\[CrossRef\]](#)
39. Cao, L.; Yang, Y.; Xue, Y.; Ma, H.; Li, Y.Y.; Hu, Y. A review of efficient nitrogen removal and phosphorus recovery by anammox-hydroxyapatite based processes: Challenges and opportunities. *J. Environ. Chem. Eng.* **2023**, *11*, 111103. [\[CrossRef\]](#)
40. Xue, Y.; Ma, H.; Kong, Z.; Li, Y.Y. Formation mechanism of hydroxyapatite encapsulation in anammox-HAP coupled granular sludge. *Water Res.* **2021**, *193*, 116861. [\[CrossRef\]](#)
41. Hu, Y.; Cheng, H.; Ji, J.; Li, Y.Y. A review of anaerobic membrane bioreactors for municipal wastewater treatment with a focus on multicomponent biogas and membrane fouling control. *Environ. Sci-Wat Res.* **2020**, *6*, 2641–2663. [\[CrossRef\]](#)
42. Song, Y.; Lin, L.; Ni, J.; Ma, H.; Qi, W.K.; Li, Y.Y. Architecture of HAP-anammox granules contributed to high capacity and robustness of nitrogen removal under 7 °C. *Water Res.* **2021**, *206*, 117764. [\[CrossRef\]](#) [\[PubMed\]](#)
43. Song, Y.; Lin, L.; Qi, W.K.; Sasaki, O.; Li, Y.Y. Anammox-mediated hydroxyapatite granules: Physicochemical properties, 3D hierarchy, and biofilm thickness. *Environ. Sci. Technol.* **2023**, *57*, 10242–10251. [\[CrossRef\]](#) [\[PubMed\]](#)
44. Pérez, J.; Laurenzi, M.; van Loosdrecht, M.C.; Persson, F.; Gustavsson, D.J. The role of the external mass transfer resistance in nitrite oxidizing bacteria repression in biofilm-based partial nitrification/anammox reactors. *Water Res.* **2020**, *186*, 116348. [\[CrossRef\]](#)
45. Kang, P.; Liang, Z.; Zhang, Q.; Zheng, P.; Yu, G.; Cui, L.; Liang, Y. The optimum particle size of anaerobic ammonia oxidation granular sludge under different substrate concentrations. *J. Environ. Manag.* **2023**, *328*, 116992. [\[CrossRef\]](#)
46. Xue, Y.; Ma, H.; Hu, Y.; Kong, Z.; Li, Y.Y. Microstructure and granulation cycle mechanisms of anammox-HAP coupled granule in the anammox EGSB reactor. *Water Res.* **2022**, *210*, 117968. [\[CrossRef\]](#)
47. Lu, D.; Gong, H.; Diao, S.; Shi, W.; Yin, R.; Dai, X. Enhanced sludge settlement of two stage PN/Anammox for reject water treatment with respective diatomite addition. *Sci. Total Environ.* **2023**, *877*, 162784. [\[CrossRef\]](#)
48. Xiao, W.; Hu, Y.; Li, S.; Shi, J.; Tian, W.; Xue, Y.; Chen, R. Operational characteristics and phosphorus recycling potential of a hydroxyapatite (HAP)-anammox process at high nitrogen loading rate. *J. Environ. Chem. Eng.* **2025**, *13*, 115759. [\[CrossRef\]](#)
49. Lan, Y.; Li, X.; Du, R.; Fan, X.; Cao, S.; Peng, Y. Hydroxyapatite (HAP) formation in acetate-driven partial denitrification process: Enhancing sludge granulation and phosphorus removal. *Sci. Total Environ.* **2023**, *903*, 166659. [\[CrossRef\]](#)
50. Fan, J.; Du, R.; Liu, Q.; Li, C.; Peng, Y. Insight into the microbial interactions of Anammox and heterotrophic bacteria in different granular sludge systems: Effect of size distribution and available organic carbon source. *Bioresour. Technol.* **2022**, *364*, 128055. [\[CrossRef\]](#)
51. Shirazi, S.; Lin, C.J.; Chen, D. Inorganic fouling of pressure-driven membrane processes—A critical review. *Desalination* **2010**, *250*, 236–248. [\[CrossRef\]](#)
52. Ali, M.; Okabe, S. Anammox-based technologies for nitrogen removal: Advances in process start-up and remaining issues. *Chemosphere* **2015**, *141*, 144–153. [\[CrossRef\]](#) [\[PubMed\]](#)
53. Wei, Y.; Xia, W.; Qian, Y.; Rong, C.; Ye, M.; Chen, Y.; Li, Y.Y. Revealing microbial compatibility of partial nitrification/Anammox biofilm from sidestream to mainstream applications: Origins, dynamics, and interrelationships. *Bioresour. Technol.* **2025**, *418*, 131963. [\[CrossRef\]](#) [\[PubMed\]](#)
54. Zhao, Y.; Feng, Y.; Chen, L.; Niu, Z.; Liu, S. Genome-centered omics insight into the competition and niche differentiation of *Ca. Jettenia* and *Ca. Brocadia* affiliated to anammox bacteria. *Appl. Microbiol. Biot.* **2019**, *103*, 8191–8202. [\[CrossRef\]](#)
55. Wu, P.; Chen, J.; Garlapati, V.K.; Zhang, X.; Jenario, F.W.V.; Li, X.; Zhang, X. Novel insights into Anammox-based processes: A critical review. *Chem. Eng. J.* **2022**, *444*, 136534. [\[CrossRef\]](#)
56. Lawson, C.E.; Wu, S.; Bhattacharjee, A.S.; Hamilton, J.J.; McMahon, K.D.; Goel, R.; Noguera, D.R. Metabolic network analysis reveals microbial community interactions in anammox granules. *Nat. Commun.* **2017**, *8*, 15416. [\[CrossRef\]](#)

Disclaimer/Publisher’s Note: The statements, opinions and data contained in all publications are solely those of the individual author(s) and contributor(s) and not of MDPI and/or the editor(s). MDPI and/or the editor(s) disclaim responsibility for any injury to people or property resulting from any ideas, methods, instructions or products referred to in the content.